南京航空航天大学

论文集

（二〇〇八年） 第21册

信息科学与技术学院

（第1分册）

上册

南京航空航天大学科技部编

二〇〇九年五月

信息科学与技术学院

041～044～045 系

上册

信息科学与技术学院2008年发表论文明细表

序号	姓名	职称	单位	论文题目	刊物、会议名称	年、卷、期
81	虞相宾	副高	042	Receiver Scheme for Space-time Coded CDMA System with Multiple Antennae	在2008年the 8th IEEE International Sysmposium on Antennas, Propagation, and EM Theory会议上交流	
82	张刚兵 刘渝 刘宗敏	博士生 教授 硕士生	042 042 042	基线比值法相位解模糊算法	南京航空航天大学学报	2008年40卷5期
83	庄丽君 王立松	硕士生 副教授	042 042	A Cluster-Interval-Based Algorithm for Optimizing Range Query in Wireless Sensor Network	在2008年 CSSE2008会议上交流	
84	李勇 朱岱寅 朱兆达	副高 教授 教授	042 042 042	An Improved Subaperture Algorithm for Airborne SAR Imaging Under Arbitrary Aircraft Maneuvers	在2007年1st Asian and Pacific Conference on Synthetic Aperture Radar 会议上上交流	
85	李勇 朱岱寅	副高 教授	042 042	Subaperture Algorithm for Airborne Spotlight SAR Imaging with nonideal motions	在2007年亚洲光电子会议上交流	
86	周沁 丁秋林	博士生 教授	042 042	Latent Supportive Utility of Irrelevent Attributes in Feature Selection	西南交通大学学报（英文版）	2008年01期
87	周日贵 丁秋林	博士生 教授	042 042	基于量子傅里叶变换的模式特征提取算法	南京航空航天大学学报	2008年01期
88	王有远 丁秋林	博士生 教授	042 042	基于风险和稳健决策的产品设计链伙伴选择	控制与决策	2008年2期
89	曹永忠 丁秋林	中级 教授	042 042	Web服务流的在线分析与动态平衡	兰州大学学报（自然科学学报）	2008年01期
90	李领治 丁秋林	博士生 教授	042 042	基于遗传算法的QoS选播流路由优化算法	计算机工程	2008年06期
91	王金栋 丁秋林	博士生 教授	042 042	一种分布式数据流系统负载平衡算法	计算机工程	2008年4期
92	周日贵 丁秋林	博士生 教授	042 042	量子Hopfied神经网络及图像识别	中国图像图形学报	2008年1期
93	杨淑群 丁秋林	副高 教授	042 042	求解简化Q矩阵的扩张算法	兰州大学学报	2008年03期
94	陈兵 丁秋林	副高 教授	042 042	分布式防火墙中的访问控制策略模型	应用科学学报	2008年3期
95	丁秋林	正高	42	信息化建设中的人文观	电气制造	2008年07期

96	丁秋林	正高	42	企业信息化道路	电气制造	2008年12期
97	曹永忠 丁秋林	中级 教授	042 042	基于公平性的服务流动态集成	计算机集成制造系统	2008年14卷12期
98	杨淑群 丁秋林	副高 教授	042 042	基于FCA具有认知诊断功能CAT的设计与实现	南京航空航天大学学报	2008年40卷5期
99	姜楠 丁秋林	博士生 教授	042 042	Power-aware Anycast Routing in Wireless Sensor Network Exploiting Small Word Effect	西南交通大学学报（英文版）	2008年4期
100	张磊 谢强 丁秋林	博士生 讲师 教授	042 042 042	语义驱动的Ontology聚类	哈尔滨工业大学学报	2008年7期
101	曹丽娟 谢强 丁秋林	硕士生 讲师 教授	042 042 042	基于分布式数据缓存技术的Web_OLAP系统研究	计算机应用	2008年2期
102	黄卫东 谢强 丁秋林	副高 讲师 教授	042 042 042	基于ART_2神经网络的设计知识需求研究	机械科学与技术	2008年3期
103	巫红霞 谢强	中级 副教授	042 042	基于有向图的频繁集挖掘算法	湖州师范学院学报	2008年01期
104	马慧 谢强	硕士生 副教授	042 042	基于GSMModem终端的短信系统研究与实现	中国制造业信息化	2008年11期
105	刘宁 谢强 丁秋林	硕士生 讲师 教授	042 042 042	基于Ontology和工作流的主动式应用服务系统	中国制造业信息化	2008年19期
106	周良 谢强 丁秋林	副高 讲师 教授	042 042 042	基于图匹配的工程图纸检索	南京航空航天大学学报	2008年3期
107	周良 谢强 丁秋林	副高 讲师 教授	042 042 042	基于草图的工程图纸检索条件输入	南京理工大学学报（自然科学版）	2008年32卷4期
108	刘豫徽 周良	硕士生 副教授	042 042	基于Agent的主动式知识服务系统	中国制造业信息化	2008年19期
109	黄科文 郑洪源 丁秋林	硕士生 副教授 教授	042 042 042	移动Agent系统JADE_S的研究与改进	计算机技术与发展	2008年03期
110	姜楠 郑洪源 丁秋林	博士生 副教授 教授	042 042 042	无线传感器网络中的局域世界演化模型	现代电子技术	2008年2期
111	王艳歌 郑洪源 丁秋林	硕士生 副教授 教授	042 042 042	基于CELTS和知识点的自主学习导航系统的设计	计算机时代	2007年1期
112	朱秋明 徐大专 陈小敏	中级 教授 讲师	042 042 042	基于IEEE802.16OFDM系统时间同步算法	西北大学学报	2008年38卷177期

113	张君 黎宁 Y.F.Li	硕士生 副高 副高	042 042 外	The Detection of Multiple Moving Objects Using Fast Level Set Method	在2008年IEEE World Congress on Computational Intelligence会议上交流	
114	夏正友	副高	042	Fighting criminals :Adaptive inferring and choosing the next investigative objects in the criminal network	Knowledge-Based Systems	2008年21卷5期
115	陆慧 夏正友	硕士生 副教授	042 042	AWT:Aspiration with Timer Search Algorithm in Siguo	Computers and Games2008	2008年10卷
116	陈小敏 徐大专 虞湘宾	中级 教授 副教授	042 042 042	Adaptive Transmit Power Allocation Scheme for V-BLAST System under Imperfect Channel State Information	在2008年The 8th International Sysmposium on Antennas, Propagation, and EM Theory会议上交流	
117	陈小敏 徐大专 虞湘宾	中级 教授 副教授	042 042 042	基于软干扰抵消的Turbo-BLAST迭代检测算法	四川大学学报（工程科学版）	2008年40卷5期
118	陈小敏 徐大专 虞湘宾	中级 教授 副教授	042 042 042	高阶调制下Turbo-BLAST系统性能	数据采集与处理	2008年23卷6期
119	汪飞	副高	042	色噪声背景下基于四元数MUSIC方法的矢量阵列信号参量估计	通信学报	2008年29卷5期
120	是莺 张小飞	硕士生 副高	042 042	quadrilinear decomposition-based blind signal detection for polarization sensitive uniform square array	Progress In Electromagnetics Research	2008年87卷
121	张小飞 徐大专	副高 教授	042 042	基于斜投影的波束形成算法	电子与信息学报	2008年30卷3期
122	张小飞 是莺 徐大专	副高 硕士生 教授	042 042 042	novel blind joint direction of arrival and polarization estemation for polarization-sensitive uniform circular array	Progress In Electromagnetics Research	2008年86卷
123	张小飞 徐大专	副高 教授	042 042	deterministic blind beamforming for electromagnetic vector sensor array	Progress In Electromagnetics Research	2008年84卷

124	张小飞 徐大专	副高 教授	042 042	blind source separation for two-dimension spread spectrum system based on trilinear decomposion	Journal of Circuits, Systems, and Computers	2008年17卷2期
125	张小飞 汪自清 徐大专	副高 本科生 教授	042 042 042	wavelet packet transform-based least mean square beamformer with low complexity	Progress In Electromagnetics Research	2008年86卷
126	张小飞 汪自清 徐大专	副高 硕士生 教授	042 042 042	Blind Joint Symbol Detection and DOA Estimation for OFDM System with Antenna Array	Wireless Pers Commun	2008年46卷
127	张小飞 余俊 冯高鹏 徐大专	副高 硕士生 本科生 教授	042 042 042 042	blind direction of arrival estimation of coherent sources using multi-invariance property	Progress In Electromagnetics Research	2008年88卷
128	张小飞 王大元 徐大专	副高 硕士生 教授	042 042 042	novel blind joint direction of arrival and frequency estemation for e uniform linear array	Progress In Electromagnetics Research	2008年86卷
129	米志超 鲍民权 周建江	博士后 副教授 教　授	042 外 042	传感器网络中基于模糊决策的多目标路由优化算法	西安电子科技大学学报	2008.35.04
130	米志超 周建江	博士后 教　授	042 042	一种启发式能量优化的无线传感器网络数据收集算法	武汉大学学报（理学版）	2008.54.03
131	米志超 周建江	博士后 教　授	042 042	带约束的多目标优化的无线传感器网络路由算法	应用科学学报	2008.26.03
132	米志超 周建江	博士后 教　授	042 042	无线传感网络中神经网络路由算法	南京航空航天大学学报	2008.40.06
133	武小红 周建江	博士生 教　授	042 042	可能性模糊C-均值聚类新算法	电子学报	2008.36.10
134	武小红 周建江	博士生 教　授	042 042	Modified possibilistic clustering model based on kernel methods	Journal os Shanghai University(English Edition)	2008.12.02
135	王　菁 周建江	博士生 教　授	042 042	一种基于GTD模型的目标散射中心提取方法	系统工程与电子技术	2008.30.11
136	武小红 周建江	博士生 教　授	042 042	基于聚类中心分离的模糊聚类模型	华南理工大学学报	2008.36.04

Receiver Scheme for Space-time Coded CDMA System with Multiple Antennae

Xiangbin Yu[1], Guangguo Bi[2]

[1] College of Information Science and Technology, Nanjing University of Aeronautics and Astronautics, Nanjing, China

[2] National Mobile Communications Research Laboratory Southeast University, Nanjing, China

Abstract— **By introducing a full-rate space-time block coding (STBC) scheme, a multiuser CDMA system with full-rate STBC is presented. Meanwhile, a low-complexity multiuser receiver scheme is developed, the scheme can make full use of the complex orthogonality of STBC to simplify the high decoding complexity of the existing scheme, it has linear decoding complexity. Compared with those full-diversity space-time block coded CDMA (STBC-CDMA) systems, the presented full-rate STBC-CDMA system can realize full rate transmission, low complexity and form efficient spatial interleaving. Thus the concatenation of channel coding can effectively improve the system performance. Simulation results show that the developed scheme can achieve almost the same performance as the existing scheme. Moreover, on the condition of same system throughput and concatenation of channel code, the proposed full-rate system has lower BER than corresponding full-diversity systems**

I. INTRODUCTION

As an effective transmit diversity technique in multi-antenna system, the space-time block coding (STBC) has been widely used to combat channel fading due to its full transmit diversity and simple maximum likelihood (ML) decoding algorithm [1-3]. But in [2], it is proved that for STBC, a complex orthogonal design which provides full diversity and full rate is not possible for more than two antennae. Considering that the full rate transmission is very important to implement high data rate service [1], and low-complexity STBC decoding algorithm is necessary due to the restriction of receiver size, a low-complexity STBC scheme that can provide full data rate and partial diversity for 3 transmit antenna (3Tx) or 4Tx is developed in [4], it has full rate, low complexity and small performance loss due to partial diversity. Moreover, it can form efficient spatial interleaving. Thus concatenated with channel coding, it is superior to corresponding full-diversity codes. But the above scheme is only designed for single-user case, thus it will be not suitable for multiuser scenario in practice. Hence, it is necessary to extend the above scheme into multiuser scenario for practical purposes. In space-time coded multiuser systems, the interference sources will perform direct-proportion increase with the increase of the number of users and transmit antennae. Although a multiuser receiver scheme for space-time coded CDMA is proposed in [5] and its decorrelative receiver scheme decouple the detection of different users, the decoding complexity is exponential for each user, which will be difficult to implement in practical application. For this reason, we present a full-rate space-time block coded CDMA (STBC-CDMA) system, then by utilizing maximum ratio combining (MRC) method and complex orthogonality of STBC, develop a low-complexity multiuser receivers scheme. This full-rate system not only has superior performance from [4], but also can achieve effective multiuser interference (MUI) suppression. After decorrelating, each user has linear decoding complexity via using the developed scheme, and the system adopts the proposed low-complexity STBC scheme in [4]. So the implement complexity of our system will be much lower. Moreover, the developed scheme can be applied to the full-diversity STBC-CDMA systems based on conventional STBC schemes [2] to implement low-complexity decoding. In addition, our presented STBC-CDMA system will not affect the data rate, which is important for high data rate services.

II. FULL-RATE AND LOW-COMPLEXITY STBC SCHEME

In this section, we give the basic principle of our full-rate STBC scheme for multiple antennae [4]. Let L, N and K be positive integers, a complex orthogonal STBC is defined by a $N\times L$ transmission matrix D, every entry of which is complex linear combination of the K input symbols $x_1,\ldots,x_K$ and their conjugates $x_1^*, \ldots,x_K^*$, and the rows of D are required to be mutually complex orthogonal. N and T are the numbers of transmit antennae and time slots used to transmit K input symbols, respectively. The rate of the orthogonal code D is defined as $R_{STBC}=K/L$. For a fair comparison, we also define the system throughput as $Throughput=R_{STBC}\times R_c\times \eta$ in terms of [6], where R_c is the code rate of the channel coding, η denotes the bandwidth efficiency of modulation scheme. Based on the Alamouti encoding, we develop a complex orthogonal and full-rate STBC scheme for multiple antennae in [4]. For 3 transmit antennae, the input information bits are firstly mapping to the constellation symbols, then every four consecutive symbols (e.g. x_1, x_2, x_3, x_4) are space-time coded in terms of our designed $N\times L$ code matrix $X=[x_1\ x_2^*\ 0\ 0;\ x_2\ -x_1^*\ x_3\ -x_4^*;\ 0\ 0\ x_4\ x_3^*]$, where $N=3$, $L=4$. According to this code matrix, 4 symbols (i.e. $K=4$) are transmitted over 4 time slots ($L=4$), so the rate of the proposed code X is 4/4=1, i.e, the X code has unity rate, thus it can realize full data rate transmission. Moreover, the rows of X keep complex orthogonal mutually, i.e., for $i\neq j$, $\mathbf{x}_i^H\cdot\mathbf{x}_j=0$; where $\mathbf{x}_i$ and $\mathbf{x}_j$ are row vectors, superscript '*' and '^{H}' denote complex conjugate and Hermitian transpose, respectively. Thus our scheme can implement full-rate and complex orthogonal design. Moreover,

This paper is supported by the startup fund of Nanjing University of Aeronautics and Astronautics (S0855-041)

978-1-4244-2193-0/08/$25.00 ©2008 IEEE

the scheme can form efficient spatial interleaving in quasi-static fading channel, which is difficult to obtain for those full-diversity STBC. So when channel coding is applied to our code scheme, the spatial interleaving effect will become very obvious and high performance gain will be obtained by the application of the inherent advantage of channel coding after utilizing the effective spatial interleaving.

III. Receiver Scheme for Full-rate Space-time coded CDMA System

In this section, we consider synchronous CDMA communication system with N transmit antennae and M receive antennae and U active users in a Rayleigh flat-fading environment, the uplink performance is investigated. To make full use of the advantage of the scheme in [4], we will consider the synchronous CDMA system comprising 3Tx and 1Rx for analysis consistency. Other cases can be investigated by using similar analytical method. The system employs the proposed full-rate STBC [4] to transmit the data from different antennae. The channel is assumed to be a quasi-static fading so that the channel gains keep constant over a frame and vary from one frame to another. The channel gains are modelled as samples of independent complex Gaussian random variables with unit-variance and zero-mean. The time block length L of STBC corresponds to P chip periods. Then according to [5], the transmitted signal matrix from 3 transmit antennae of user u at pth (p=1,2,...,P) chip period is

$$\boldsymbol{S}_u(p) = \boldsymbol{D}_u \boldsymbol{C}_u(p) \tag{1}$$

where $\boldsymbol{D}_u$ is $3\times L$ STBC matrix of user u, $\boldsymbol{C}_u(p)$ is $L\times 1$ spreading code, and $\boldsymbol{C}_u=[\boldsymbol{C}_u(1),...,\boldsymbol{C}_u(P)]$ corresponds to L normalized spreading codes of length P used to spread $\boldsymbol{D}_u$ for user u (u=1,2,...U), such as conventional Walsh-Hadamard code and Gold code. We will also employ these different spreading codes for different users. Based on the analytical method in [5], at the receiver, we can obtain the baseband received signal at p th (p=1,2,...,P) chip period as follows:

$$R(p) = \sum_{u=1}^{U} \sqrt{\lambda_u}\, \boldsymbol{h}_u \boldsymbol{S}_u(p) + z(p), \quad p=1,...,P \tag{2}$$

where $\boldsymbol{h}_u=[h_{u1}, h_{u2}, h_{u3}]$ is 1×3 channel matrix of user u, and its elements $\{h_{un}, n=1,2,3\}$denote complex channel gains from transmit antenna n to receive antenna. $z(p)$, p=1,2,...,P are independent, identically distributed complex Gaussian random variables with zero-mean and unit-variance. $N\lambda_u$ denotes the average signal-to-noise ratio (SNR) per receive antenna for user u at the receiver during the transmission of STBC matrix $\boldsymbol{D}_u$ (which corresponds to P chip periods), this SNR adopts the definition similar to Ref.[5] for comparison consistency.

Based on the above analysis, the proposed full-rate STBC, i.e. X code is employed for $\boldsymbol{D}_u$. Then according to (2) and (1), the received signal at pth chip period can be expressed as

$$R(p)=\sum_{u=1}^{U}\sqrt{\lambda_u}\,[h_{u1}\ h_{u2}\ h_{u3}]\begin{bmatrix} x_{u1} & x_{u2}^* & 0 & 0 \\ x_{u2} & -x_{u1}^* & x_{u3} & -x_{u4}^* \\ 0 & 0 & x_{u4} & x_{u3}^* \end{bmatrix}\boldsymbol{C}_u(p)+z(p) \tag{3}$$

where p=1,2,...,P, L=4; $\{x_{uk}, k=1,...,4\}$are the transmitted data symbols for user u, they are from energy-normalized signal constellation Ω.

In order to express (3) more compactly, we simplify its general form, i.e. Eq.(2), and define the following matrices:

$\boldsymbol{B}_u=\lambda_u^{1/2}\boldsymbol{h}_u\boldsymbol{D}_u$ ($1\times L$ matrix); $\boldsymbol{B}=[\boldsymbol{B}_1, \boldsymbol{B}_2,...,\boldsymbol{B}_U]$ ($1\times LU$ matrix); $\boldsymbol{C}_u=[\boldsymbol{C}_u(1),...,\boldsymbol{C}_u(P)]$ ($L\times P$ matrix); $\boldsymbol{C}=[\boldsymbol{C}_1^T,...,\boldsymbol{C}_U^T]^T$, ($LU\times P$ matrix); $\boldsymbol{R}=[R(1),...,R(P)]$ ($1\times P$ matrix); $\boldsymbol{Z}=[z(1),..., z(P)]$, corresponds to $1\times P$ matrix, where superscript 'T' denotes transpose of matrix. Thus, (2) becomes

$$\boldsymbol{R}=\sum_{u=1}^{U}\boldsymbol{B}_u\boldsymbol{C}_u+\boldsymbol{Z}=\boldsymbol{B}\boldsymbol{C}+\boldsymbol{Z} \tag{4}$$

Then according to Ref.[7], we can obtain the ML estimate of $\boldsymbol{B}$ conditioned on $\{\boldsymbol{h}_u, u=1,...,U\}$ and $\{\boldsymbol{D}_u, u=1,...,U\}$as

$$\hat{\boldsymbol{B}}=\boldsymbol{R}\boldsymbol{C}^{\mathrm{H}}(\boldsymbol{C}\boldsymbol{C}^{\mathrm{H}})^{-1}=\boldsymbol{B}+\boldsymbol{Z}\boldsymbol{C}^{\mathrm{H}}(\boldsymbol{C}\boldsymbol{C}^{\mathrm{H}})^{-1} \tag{5}$$

Here, the Moore-Penrose inverse matrix $\boldsymbol{C}^{\mathrm{H}}(\boldsymbol{C}\boldsymbol{C}^{\mathrm{H}})^{-1}$ can be expressed as a multiuser decorrelator [5,7], thus the ML estimate $\hat{\boldsymbol{B}}$ is effective output of the decorrelator with the input being the received data $\boldsymbol{R}$. By this decorrelator, the multiuser interference is cancelled, and the detection of different users is decoupled. Based on the block structure of $\boldsymbol{B}$, the ML estimate $\hat{\boldsymbol{B}}_u$ of $\boldsymbol{B}_u$ can be easily achieved. According to the definition of $\boldsymbol{B}_u$, we can assume that $\hat{\boldsymbol{B}}_u=[\hat{b}_{u1}, \hat{b}_{u2}, ...,\hat{b}_{uL}]$. Thus for (3), which corresponds to our proposed full-rate STBC scheme, L=4 and $\hat{\boldsymbol{B}}_u=[\hat{b}_{u1}, \hat{b}_{u2}, \hat{b}_{u3}, \hat{b}_{u4}]$. Considering that the transmitted information symbols constitute the code matrix $\boldsymbol{D}_u$, and $\boldsymbol{D}_u$ is contained in matrix $\boldsymbol{B}_u$, the symbol decision values can be achieved by evaluating $\hat{\boldsymbol{B}}_u$. Moreover, we find that the $\boldsymbol{B}_u$ has same receiver signal form as conventional STBC in single user scenario [4,8]. Thus based on the MRC method, utilizing the complex orthogonality of STBC, we can obtain simple decoding scheme of user u for the proposed full-rate STBC-CDMA system at the receiver after performing decorrelation, i.e.,

$$\begin{cases} \hat{x}_{u1}=\arg\min\limits_{x_{u1}\in\Omega}\| h_{u1}^*\hat{b}_{u1}-h_{u2}\hat{b}_{u2}^*-\sqrt{\lambda_u}(|h_{u1}|^2+|h_{u2}|^2)x_{u1}\|^2 \\ \hat{x}_{u2}=\arg\min\limits_{x_{u2}\in\Omega}\| h_{u2}^*\hat{b}_{u1}+h_{u1}\hat{b}_{u2}^*-\sqrt{\lambda_u}(|h_{u1}|^2+|h_{u2}|^2)x_{u2}\|^2 \\ \hat{x}_{u3}=\arg\min\limits_{x_{u3}\in\Omega}\| h_{u2}^*\hat{b}_{u3}+h_{u3}\hat{b}_{u4}^*-\sqrt{\lambda_u}(|h_{u2}|^2+|h_{u3}|^2)x_{u3}\|^2 \\ \hat{x}_{u4}=\arg\min\limits_{x_{u4}\in\Omega}\| h_{u3}^*\hat{b}_{u3}-h_{u2}\hat{b}_{u4}^*-\sqrt{\lambda_u}(|h_{u2}|^2+|h_{u3}|^2)x_{u4}\|^2 \end{cases} \tag{6}$$

By introducing 3-antenna full-diversity STBC G_3 and H_3 code, the corresponding full-diversity STBC-CDMA systems can be given. Based on the above analysis method, we can obtain the receiver decoding scheme for 3-antenna G_3 code based multiuser CDMA system after decorrelation. Namely, for G_3 code, L=8, K=4; we have

$$
\begin{cases}
\hat{x}_{u1} = \arg\min\limits_{x_{u1}\in\Omega} \| \hat{b}_{u1}h_{u1}^{*} + \hat{b}_{u2}h_{u2}^{*} + \hat{b}_{u3}h_{u3}^{*} + \hat{b}_{u5}^{*}h_{u1} + \hat{b}_{u6}^{*}h_{u2} + \hat{b}_{u7}^{*}h_{u3} \\
\qquad -2\sqrt{\lambda_u}(|h_{u1}|^2 + |h_{u2}|^2 + |h_{u3}|^2)x_{u1} \|^2 \\
\hat{x}_{u2} = \arg\min\limits_{x_{u2}\in\Omega} \| \hat{b}_{u1}h_{u2}^{*} - \hat{b}_{u2}h_{u1}^{*} + \hat{b}_{u4}h_{u3}^{*} + \hat{b}_{u5}^{*}h_{u2} - \hat{b}_{u6}^{*}h_{u1} + \hat{b}_{u8}^{*}h_{u3} \\
\qquad -2\sqrt{\lambda_u}(|h_{u1}|^2 + |h_{u2}|^2 + |h_{u3}|^2)x_{u2} \|^2 \\
\hat{x}_{u3} = \arg\min\limits_{x_{u3}\in\Omega} \| \hat{b}_{u1}h_{u3}^{*} - \hat{b}_{u3}h_{u1}^{*} - \hat{b}_{u4}h_{u2}^{*} + \hat{b}_{u5}^{*}h_{u3} - \hat{b}_{u7}^{*}h_{u1} - \hat{b}_{u8}^{*}h_{u2} \\
\qquad -2\sqrt{\lambda_u}(|h_{u1}|^2 + |h_{u2}|^2 + |h_{u3}|^2)x_{u3} \|^2 \\
\hat{x}_{u4} = \arg\min\limits_{x_{u4}\in\Omega} \| \hat{b}_{u3}h_{u2}^{*} - \hat{b}_{u2}h_{u3}^{*} - \hat{b}_{u4}h_{u1}^{*} - \hat{b}_{u6}^{*}h_{u3} + \hat{b}_{u7}^{*}h_{u2} - \hat{b}_{u8}^{*}h_{u1} \\
\qquad -2\sqrt{\lambda_u}(|h_{u1}|^2 + |h_{u2}|^2 + |h_{u3}|^2)x_{u4} \|^2
\end{cases} \quad (7)
$$

For space consideration, we no longer give the decoding scheme for 3-antenna full-diversity H_3 code based CDMA system due to the repeated work.

From the Eqs.(6) and (7), it is observed that our improved decoding scheme has linear complexity. For Ref.[5], its receiver decoding schemes with coherent detection (i.e. (44) and (45) in [5]) are shown as follows:

1) For general spreading codes:

$$\hat{\boldsymbol{D}}_u = \arg\min_{\{x_{u1},\ldots,x_{uK}\}\in\Omega} \{\mathrm{vec}^H(\hat{\boldsymbol{B}}_u - \sqrt{\lambda_u}\boldsymbol{h}_u\boldsymbol{D}_u)\Phi_u^{-1}\mathrm{vec}(\hat{\boldsymbol{B}}_u - \sqrt{\lambda_u}\boldsymbol{h}_u\boldsymbol{D}_u)\} \quad (8)$$

2) For orthogonal spreading codes:

$$\hat{\boldsymbol{D}}_u = \arg\min_{\{x_{u1},\ldots,x_{uK}\}\in\Omega} \|\hat{\boldsymbol{B}}_u - \sqrt{\lambda_u}\boldsymbol{h}_u\boldsymbol{D}_u\|_F^2 \quad (9)$$

From the above two equations, we can see that the decoding scheme in [5] has exponential complexity. Namely, if Ω is a constellation consists of Q symbols, the search times that need to obtain the transmitted K symbols is Q^K. Thus, when Q and K become larger, the complexity will get much higher, which will result in the significant increase of implementation complexity of the system. While for our improved scheme, the needed search times are only KQ. Based on this, we give the complexity comparison between the improved scheme and the original scheme [5] in Table I. In Table I, scheme 1 and scheme 2 represent the original decoding scheme [5] and our improved scheme, respectively. From the Table, we observe that scheme 2 has lower complexity than scheme 1. Especially, when Q and K are larger, the low-complexity advantage of our scheme becomes more significant.

TABLE I
COMPLEXITY COMPARISON BASED ON SEARCH TIMES

	QPSK Q=4, K=2	8PSK Q=8, K=2	16QAM Q=16, K=3	16QAM Q=16, K=4
Scheme 1	16	64	4096	65536
Scheme 2	8	16	48	64

In addition, the above proposed decoding method can be easily extended to multiple receive antennae case. Here, we no longer give detailed decoding process due to the similar work and space consideration.

IV. SIMULATION RESULTS

In this section, we will provide the performance simulation results for different STBC-CDMA systems, and the G_2, G_3 code and proposed full-rate X code are investigated and compared. In simulation, the channel is assumed to be quasi-static Rayleigh flat fading; the receiver has perfect channel knowledge and system synchronization. Every data frame includes 480 information bits, and Gray mapping of the bits to symbol is employed. For different STBCs, we will adopt different modulation modes to maintain the same system throughput. 7-user synchronous CDMA systems are considered, and conventional Gold codes (P=63) are used as spreading code. Considering that turbo code has good decoding performance, we employ turbo code as channel coding to improve the system performance. The turbo code consists of two identical recursive systematic convolutional codes (1, G_n/G_d) connected in parallel via a pseudorandom interleaver, where G_n and G_d are chosen to be 15_{octal} and 13_{octal}, respectively. The code rate R_c =1/3, and the maximum a posteriori probability (MAP) is used for turbo decoding, the number of iterations is 5. The simulation results are illustrated in Figs.1-2, respectively. In the figures, 'G_2-CDMA', 'G_3-CDMA', 'X-CDMA' denote the CDMA systems with G_2 code, G_3 code and proposed full-rate STBC, respectively.

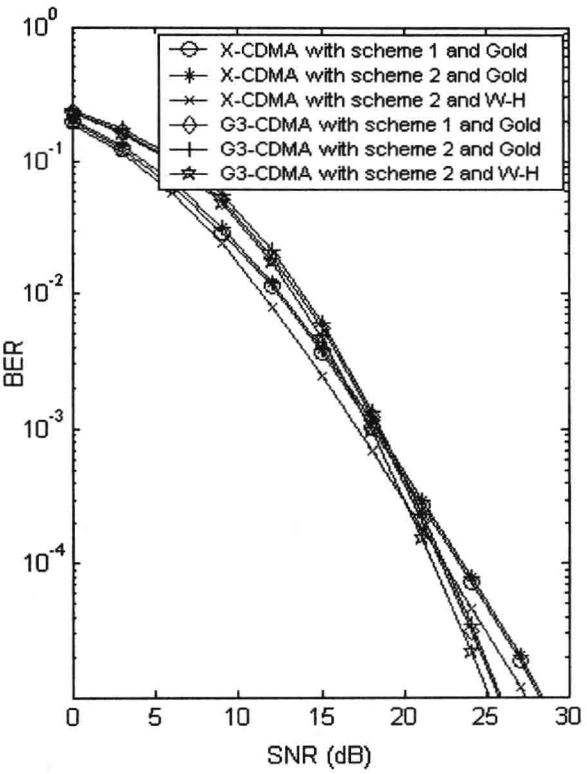

Fig. 1 BER versus SNR for different STBC-CDMA systems

Fig.1 shows the BER versus SNR for different STBC-CDMA systems. The QPSK modulation is employed in conjunction with full-rate STBC-CDMA system, and the

16QAM modulation is applied to G_3-CDMA system. Thus the system throughputs all equal 2 bit/s/Hz. For comparison, we also give the performance of different STBC-CDMA systems with spreading code being Walsh-Hadamard (W-H) code (P=64), and the performance of different STBC-CDMA with scheme 1 (i.e., the original scheme [5]). It is shown in Fig.1 that our full-rate STBC-CDMA system outperforms the G_3-CDMA system at low SNR, but performs worse than G_3-CDMA system at high SNR whether with Gold code or with W-H code due to partial diversity. Besides, the system performance with orthogonal W-H code is slightly superior to that with Gold code. The reason for this is that the Gold codes are quasi-orthogonal, and can not cancel the MUI completely, thus bring about less than 1 dB performance loss. Moreover, from the Fig.1, we can see that multiuser STBC-CDMA system with scheme 2 (i.e. our decoding scheme) has almost the same performance as multiuser STBC-CDMA system with scheme 1, but the implement complexity of scheme 2 is much lower than scheme 1.

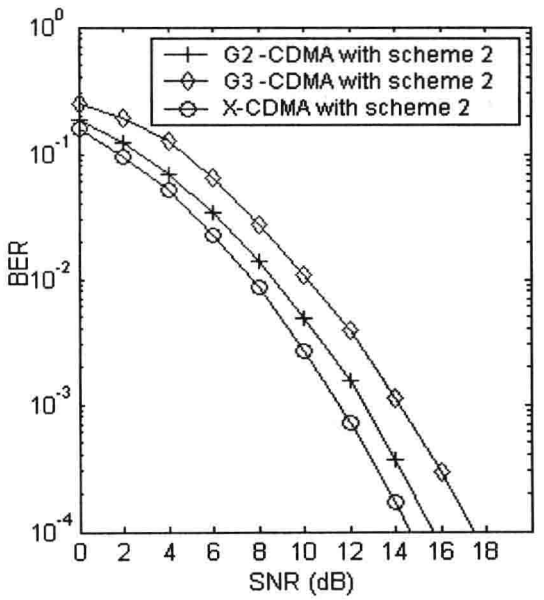

Fig. 2 BER versus SNR for different STBC-CDMA systems with turbo coding

In Fig.2, we compare the performance of different STBC-CDMA systems concatenated with turbo coding, and low-complexity scheme 2 is used for simple decoding. In Fig.2, the G_2 code, G_3 code and the full-rate X code are employed. For G_2-CDMA system and the proposed STBC-CDMA system, QPSK modulation is used, while for G_3-CDMA system, the 16QAM modulation is adopted. Thus the system throughput with turbo coding is 2/3bit/s/Hz. As shown in Fig.3, the proposed STBC-CDMA system has superior performance over full-diversity G_3-CDMA system and G_2-CDMA system. On the condition of same throughput, the proposed system gives about 2.5 dB gains over G_3-CDMA system and 1.5 dB over G_2-CDMA system at a BER of 10^{-4}, respectively. This is because our full-rate code scheme can form effective spatial interleaving. Thus corresponding system performance is significantly improved when concatenated with channel coding. Besides, the more vulnerable 16QAM scheme is used for low-rate G_3-CDMA system to maintain the same throughput, whereas the 16QAM constellation points are more densely packed when compared with QPSK, thus they are more prone to errors in fading channel. As a result, the performance of G_3-CDMA system will be affected greatly.

V. Conclusions

We have given a full-rate STBC-CDMA system model and developed a simple and effective multiuser receiver scheme. The scheme can effectively suppress MUI via multiuser detection method, and simplify the high decoding complexity of the existing scheme by utilizing the complex orthogonality of STBC. Compared to the existing scheme with exponential decoding complexity, our scheme has linear decoding complexity and can achieve almost the same performance as the existing scheme. Moreover, compared with full-diversity and low-rate multiuser CDMA systems, our full-rate multiuser CDMA system can realize full data rate transmission and low complexity, and form efficient spatial interleaving. Simulation results show that on the condition of same system throughput and concatenation of channel code, the proposed full-rate STBC-CDMA system has lower BER than the full-diversity STBC-CDMA systems. So our system scheme has not only superior performance but also low implement complexity.

References

[1] H.Jafarkhani, "A quasi-orthogonal space-time block code", *IEEE Trans. Commun.*, vol.49, no.1, pp.1-4, 2001

[2] V.Tarokh, H.Jafarkhani, A.R.Calderbank, "Space-time block codes from orthogonal designs", *IEEE Trans. Inform. Theory*, Vol.45, pp.1456-1467, 1999.

[3] S.M.Alamouti, "A simple transmit diversity technique for wireless communications", *IEEE J. Select. Areas Commun.*, Vol.16, pp.1451-1458, 1998.

[4] Xiangbin Yu, Dazhuan Xu, and Guangguo Bi, "Full-rate complex orthogonal space-time block code for multiple antennas," *Wireless Personal Communications*, vol.40, no.1, pp.81-89, 2007.

[5] Hongbin Li, Jian Li., "Differential and coherent decorrelating multiuser receivers for space-time coded CDMA systems", *IEEE Trans Signal processing*, Vol.50, pp. 2529-2536,2002.

[6] T.H.Liew, L.Hanzo, "Space-time codes and concatenated channel codes for wireless communications", *Proceedings of the IEEE*, Vol.90, pp.187-219, 2002.

[7] S.Verdu, Multiuser detection, Cambridge, U.K: Cambridge university press, 1998.

[8] V.Tarokh, H.Jafarkhani, and R.Calderbank, "Space-time block coding for wireless communications: performance results", *IEEE J. Select. Areas Commun.*, Vol.17, pp. 451-460, 1999.

第40卷第5期
2008年10月

南京航空航天大学学报
Journal of Nanjing University of Aeronautics & Astronautics

Vol 40 No. 5
Oct 2008

基线比值法相位解模糊算法

张刚兵[1] 刘 渝[1] 刘宗敏[2]

(1. 南京航空航天大学信息科学与技术学院, 南京, 210016; 2. 中航雷达与电子设备研究院, 无锡, 214063)

摘要: 研究了由$N-1$个等比值双基线系统组成的N基线测向系统的相位解模糊算法。对每个双基线系统$(P_n\frac{\lambda_0}{2}, P_{n+1}\frac{\lambda_0}{2})$在$(-p/2, p/2)$, $(-q/2, q/2)$范围内进行一维整数搜索, 寻找出一组相位模糊解(k_{0n}, l_{0n}), 根据二元一次不定方程, 得到该双基线系统的模糊解, 解的组数为P_n, P_{n+1}的最大公约数(Greatest common divisor, GCD), 然后, 寻找由$(P_1\frac{\lambda_0}{2}, P_2\frac{\lambda_0}{2}, P_3\frac{\lambda_0}{3})$构成的三基线系统的相位模糊解, 解的组数为$P_1$, P_2和P_3的最大公约数。以此类推, 可得N基线系统的相位模糊解, 如$P_1, P_2, \cdots, P_N$的最大公约数为1, 那么就可得到惟一解, 实现相位无模糊。该算法的计算量小, 便于工程实现, 仿真结果表明了算法的有效性。

关键词: 干涉仪; 基线比值恒定; 相位解模糊

中图分类号: TN 911.7 **文献标识码**: A **文章编号**: 1005-2615(2008)05-0665-05

Unwrapping Phase Ambiguity Algorithm Based on Baseline Ratio

Zhang Gangbing[1], *Liu Yu*[1], *Liu Zongmin*[2]

(1. College of Information Science and Technology, Nanjing University of Aeronautics & Astronautics, Nanjing, 210016, China; 2. Radar and Avionics Institute of Avic, Wuxi, 214063, China)

Abstract: The unwrapping phase ambiguity algorithm of N-baseline direction finding system including $N-1$ constant ratio double-baseline direction-finding subsystem is studied. One-dimensional integer search is made to find a pair of phase ambiguity number (k_{0n}, l_{0n}) within the scope of $(-p/2, p/2)$, $(-q/2, q/2)$ for each double-baseline direction finding system $(P_n\frac{\lambda_0}{2}, P_{n+1}\frac{\lambda_0}{2})$. The pairs of phase ambiguity numbers of the double-baseline are acquired according to two variables first-order indefinite equation, which are equal to the greatest common divisor (GCD) of P_n and P_{n+1}. The pairs of phase ambiguity numbers of the triple-baseline are the GCD of P_1, P_2 and P_3 through the triple-baseline system composed of $(P_1\frac{\lambda_0}{2}, P_2\frac{\lambda_0}{2}, P_3\frac{\lambda_0}{2})$. The rest can be deduced by analogy, and the sets of phase ambiguity numbers of the N-baseline are obtained. The unique set of phase ambiguity numbers can be obtained if the GCD of $P_1, P_2, \cdots, P_N$ is equal to unit. The algorithm has a low computation, thus it is suitable for real-time processing. Finally, simulation results verify its validity.

Key words: interferometers; constant ratio baseline; unwrapping phase ambiguity

引 言

相位干涉仪被广泛应用于波达角的估计领域[1-3], 在两阵元间距大于半波长时, 相位干涉仪的鉴相输出可能会出现2π模糊。文献[4]提出了一种基于孙子定理解模糊的算法, 在基线比为互素的条件下, 能对相位干涉仪的鉴相输出解模糊, 但其基线长度的选择受到了限制, 难以提高测向精度。文

收稿日期: 2007-06-07; **修订日期**: 2008-04-25

作者简介: 张刚兵, 男, 博士研究生, 1978年11月生; 刘渝(联系人), 男, 教授, 博士生导师, E-mail: liuyu_nuaa@yahoo.com.cn。

献[5]提出了一种基于参差距离的相位差解模糊算法，在基线长度满足参差关系的条件下，利用最小均方误差准则进行多维整数搜索能对相位干涉仪的鉴相输出解模糊，但该算法存在计算量大的缺点。文献[6]在文献[5]基础上提出了一种基于多组基线解模糊的算法，该算法虽然利用基线间的长度关系将多维整数搜索转化为多次的二维整数搜索，大大减少了计算量，但是采用最小均方误差准则进行二维整数搜索的计算量仍然比较大，不利于实时计算。本文在文献[6]的基础上提出了一种相位解模糊算法，该算法要求所有相邻基线长度之比为恒定互素数之比以及所有基线长度整数比的最大公约数为1。与文献[6]的算法相比较，该算法只需要进行多次一维整数搜索，它具有搜索范围窄、计算量小、算法简单等优点。

1 基线比值法解模糊的算法

1.1 干涉仪阵列相位解的结构

一维N基线相位干涉仪的结构如图1所示，图中$N+1$个两两相邻的接收阵元构成N个相位干涉仪，组成一个相位干涉仪阵列。干涉仪基线长度分别为$L_1, L_2, \cdots, L_N$，且都为最高接收频率半波长的整数倍，即$L_n = P_n \frac{\lambda_0}{2}$，$P_n$为正整数，$\lambda_0$为最高接收频率信号的波长，则基线长度之比为$L_1 : L_2 : \cdots : L_N = \left(P_1 \frac{\lambda_0}{2}\right) : \left(P_2 \frac{\lambda_0}{2}\right) : \cdots : \left(P_N \frac{\lambda_0}{2}\right) = P_1 : P_2 : \cdots : P_N$，要求各基线整数比的最大公约数(Greatest common divisor, GCD)为1，即GCD$(P_1, P_2, \cdots, P_N) = 1$。如果相邻基线长度的比值都为$p/q$($p$, q为互素的正整数)，此时基线长度之比为$L_1 : L_2 : \cdots : L_N = P_1 : P_2 : \cdots : P_N = p^{N-1} : p^{N-2}q : \cdots : q^{N-1}$。

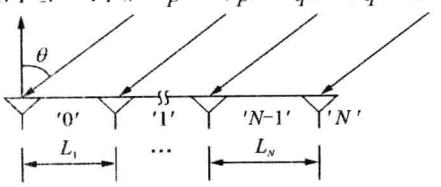

图1 一维N基线相位干涉仪原理图

在辐射源处于远场位置时，可以把来波当成平面波。设入射信号的波长为$\lambda(\lambda \geqslant \lambda_0)$，入射方向与天线视轴的夹角为$\theta$，则由入射信号波程差引起的各相位干涉仪的相位差$\varphi_n = 2\pi L_n \sin\theta/\lambda$，$n = 1, 2, \cdots, N$。测量$\varphi_n$就能得到信号波达角的估计值$\hat{\theta} = \arcsin[\varphi_n \lambda/(2\pi L_n)]$，其估计方差$\mathrm{var}(\hat{\theta}) = [\lambda/(2\pi L_n \cos\theta)]^2 \sigma_\varphi^2$，$\sigma_\varphi^2$为鉴相方差。在鉴相方差相同的条件下，波达角估计方差与基线长度的平方成反比，通常采用长基线提高估计精度。即按

$$\hat{\theta} = \arcsin\{(\varphi_1 + \varphi_2 + \cdots + \varphi_N)\lambda/[2\pi(L_1 + L_2 + \cdots + L_N)]\} \tag{1}$$

来估计波达角θ。

相位干涉仪的鉴相输出只能在主值范围$(-\pi, \pi]$内，当基线长度L_n大于半波长时，输出的鉴相值φ_n可能存在2π模糊，即

$$\varphi_n = \phi_n \bmod(2\pi),\ \phi_n = \varphi_n + 2\pi m_n \quad n = 1, 2, \cdots, N \tag{2}$$

式中m_n为整数，是基线L_n的相位模糊数。将$\phi_n = 2\pi L_n \sin\theta/\lambda$代入式(2)有

$$m_n = L_n \sin\theta/\lambda - \varphi_n/2\pi \quad n = 1, 2, \cdots, N \tag{3}$$

由于入射角度存在方向性，θ可在$(-\pi/2, \pi/2)$范围内变化，因此m_n的取值满足

$$-L_n/\lambda - \varphi_n/2\pi < m_n < L_n/\lambda - \varphi_n/2\pi \quad n = 1, 2, \cdots, N \tag{4}$$

在来波信号具有最高的接收频率时，$\lambda = \lambda_0$，此时满足式(4)的m_n具有最大的取值范围

$$-P_n/2 - \varphi_n/2\pi < m_n < P_n/2 - \varphi_n/2\pi \quad n = 1, 2, \cdots, N \tag{5}$$

因此可以将相位模糊数m_n的取值限定为在$(-P_n/2, P_n/2]$区间上的整数值。当来波信号低于最高接收频率时，m_n的取值不会超出该区间范围。此时波达角θ的估计方程可变为

$$\hat{\theta} = \arcsin\{\lambda[(\varphi_1 + \varphi_2 + \cdots + \varphi_N)/2\pi + (m_1 + m_2 + \cdots + m_N)]/(L_1 + L_2 + \cdots + L_N)\} \tag{6}$$

波达角估计的关键就是要确定式(2)中的各个相位模糊数m_n，当存在噪声时，对模糊数的求解比较复杂[7]，如果在最小均方误差准则下对式(2)组成的方程组进行N维整数搜索，计算量很大[6]，难以实时实现。

下面给出两个命题。

命题1 在不存在噪声时，分别在$(-P_n/2, P_n/2]$，$(-P_{n+1}/2, P_{n+1}/2]$范围内满足方程

$$(\varphi_n + 2\pi m_n)/(\varphi_{n+1} + 2\pi m_{n+1}) = L_n/L_{n+1} = p/q \quad n = 1, 2, \cdots, N-1 \tag{7}$$

的相位模糊数(m_n, m_{n+1})有GCD(P_n, P_{n+1})组。

命题2 在不存在噪声时，前n根基线分别在$(-P_1/2, P_1/2]$，$(-P_2/2, P_2/2]$，…，$(-P_n/2, P_n/2]$范围内可以确定GCD$(P_1, P_2, \cdots, P_n)$组相位模糊数$(m_1, m_2, \cdots, m_n)$，$n = 2, 3, \cdots, N$。

根据命题1，图1中每个双基线测向系统都能利用各自的鉴相值与它们基线长度之间的关系确定GCD(P_n, P_{n+1})组相位模糊数(m_n^n, m_{n+1}^n)，$n = 1, 2, \cdots, N-1$。(m_n^n, m_{n+1}^n)为由L_n, L_{n+1}组成的第n个双基线测向系统确定，并分别对应基线L_n, L_{n+1}的相位模糊数，在这GCD(P_n, P_{n+1})组解中只有一组

是真实的相位模糊数。

基线L_2的相位模糊数是由第1个和第2个双基线测向系统共同确定的, 因此基线L_2的相位模糊数是两个解集合(m_1^1, m_2^1), (m_2^2, m_3^2)中满足$m_{2i}^1 = m_{2j}^2$的公共解, $i \in [0, 1, \cdots, \mathrm{GCD}(P_1, P_2) - 1]$, $j \in [0, 1, \cdots, \mathrm{GCD}(P_2, P_3) - 1]$, 根据命题2, 该公共解共有$\mathrm{GCD}(P_1, P_2, P_3)$组。此时满足三基线$L_1$, L_2, L_3的相位模糊数为$(m_1, m_2, m_3) = \{(m_{1i}^1, m_{2i}^1, m_{3j}^2) \mid (m_{1i}^1, m_{2i}^1) \in (m_1^1, m_2^1), (m_{2j}^2, m_{3j}^2) \in (m_2^2, m_3^2), \text{且} m_{2i}^1 = m_{2j}^2\}$, 其中$i \in [0, 1, \cdots, \mathrm{GCD}(P_1, P_2) - 1]$, $j \in [0, 1, \cdots, \mathrm{GCD}(P_2, P_3) - 1]$。

基线L_3的相位模糊数还可以由L_3, L_4组成的第3个双基线测向系统确定, 因此其相位模糊数是两集合(m_1, m_2, m_3), (m_3^3, m_4^3)中满足$m_{3i}^3 = m_{3j}^3$的公共解, $i \in [0, 1, \cdots, \mathrm{GCD}(P_1, P_2, P_3)] - 1$, $j \in [0, 1, \cdots, \mathrm{GCD}(P_3, P_4)] - 1$, 根据命题2, 该公共解共有$\mathrm{GCD}(P_1, P_2, P_3, P_4)$组。

以此类推, 利用前n根基线的公共解就能逐步将相位模糊数缩小为$\mathrm{GCD}(P_1, P_2, \cdots, P_n)$种可能的组合, $n = 2, 3, \cdots, N$。根据给定条件$\mathrm{GCD}(P_1, P_2, \cdots, P_N) = 1$, 就能惟一确定各基线真实的相位模糊数。

1.2　双基线相位模糊数的求解

下面讨论双基线测向系统相位模糊数(m_n^n, m_{n+1}^n)的求解算法。由方程(7)可以得到

$$m_{n+1}p - m_n q = q\varphi_n/2\pi - p\varphi_{n+1}/2\pi \quad n = 1, 2, \cdots, N-1 \tag{8}$$

即

$$m_{n+1} = m_n q/p + q\varphi_n/2p\pi - \varphi_{n+1}/2\pi \quad n = 1, 2, \cdots, N-1 \tag{9}$$

在不存在噪声时, 方程(8)是整数域上的二元一次不定方程, 根据文献[8], 如果(k_n, l_n)是方程(8)的任意一组解, 那么$m_n = k_n + pt, m_{n+1} = l_n + qt$就是方程(8)的通解, t是任意整数, 且m_n, m_{n+1}的无模糊范围分别为$(-p/2, p/2)$, $(-q/2, q/2)$。如果能分别求出方程(8)在$(-p/2, p/2)$, $(-q/2, q/2)$范围内的相位模糊解(k_{0n}, l_{0n}), 那么在式(5)的约束下, 根据通解公式就能求出其他$\mathrm{GCD}(P_n, P_{n+1}) - 1$组解。此时$m_n, m_{n+1}$的搜索范围就能分别从$(-P_n/2, P_n/2]$, $(-P_{n+1}/2, P_{n+1}/2]$变为$(-p/2, p/2)$, $(-q/2, q/2)$, 可以大大缩小搜索范围。当满足正确解模糊条件时(下节讨论正确解模糊条件), 真实的相位模糊数必定包含在这$\mathrm{GCD}(P_n, P_{n+1})$组解中。

对于不定方程(9), 在$(-p/2, p/2)$范围内每给定一个整数值m_n', 在$(-q/2, q/2)$范围内就能求出一个对应的m_{n+1}'。由于噪声的存在, m_{n+1}'不是整数, 离m_{n+1}'最近的整数就是L_{n+1}在$(-q/2, q/2)$范围内的相位模糊数l_{0n}, 与之对应的m_n'就是L_n在$(-p/2, p/2)$范围内的相位模糊数k_{0n}。为了减少计算量, 提高运算速度, 可以在式(5)的约束下, 以$m_{n0} = k_{0n}$为初始条件, 分别按$m_{n(j+1)} = m_{nj} + p$, $m_{n(j+1)} = m_{nj} - p$递推求基线L_n在正、负半轴上的相位模糊数。同样, 以$m_{(n+1)0} = l_{0n}$为初始条件, 分别按$m_{(n+1)(i+1)} = m_{(n+1)i} + q$, $m_{(n+1)(j+1)} = m_{(n+1)j} - q$递推可求$L_{n+1}$在正、负半轴上的相位模糊数。

在双基线L_n, L_{n+1}长度比的最大公约数大于1时, 可以分别在区间$(-p/2, p/2)$, $(-q/2, q/2)$上求满足方程(9)的解(k_{0n}, l_{0n}), 再利用解之间的模糊关系得到其他相位模糊数, 然后利用多组基线的公共解, 就能逐步缩小相位模糊数的组合范围。当多组基线长度比的最大公约数为1时, 只有真实的一组相位模糊数才能同时满足方程(7)。基于这种考虑, 本文提出了基线比值法多组相位解模糊的算法, 只需在双基线无模糊范围内进行多次一维整数搜索, 其计算量较小。

1.3　解模糊步骤

先由双基线测向系统确定各基线可能的相位模糊数, 再利用公共解逐步缩小解的范围, 最后确定真实的相位模糊数, 算法的具体步骤为:

(1) 对每一个双基线系统进行解模糊处理, 确定相位模糊数m_n, m_{n+1}的$\mathrm{GCD}(P_n, P_{n+1})$种组合, 记为$(m_n^n, m_{n+1}^n)$, $n = 1, 2, \cdots, N-1$。

(2) 从相位模糊数组合中找出同时满足$m_{n+1}^n = m_{n+1}^{n+1}$的一组模糊解$m_1, m_2, \cdots, m_N$, $n = 1, 2, \cdots, N-1$, 那么$m_1, m_2, \cdots, m_N$就是各相位干涉仪鉴相输出的真实相位模糊数。

(3) 求无模糊的相位差$\Phi = \varphi + 2\pi m_n$, $n = 1, 2, \cdots, N$, 从而得到波达角的估计值。

该算法的关键在于第(1)步, 它在最小的搜索范围内确定了满足方程(9)的相位模糊数, 使得在求解其他相位模糊数时省去了大量的搜索过程。整个算法过程只需要进行$N-1$次一维整数搜索, 计算量小, 适合实时计算。

1.4　算法计算量分析

从算法的整个实现过程来看, 本文算法只需要在双基线的无模糊范围内进行一维整数搜索, 因此计算量很小。为了便于统计计算量, 将除法与乘法统一成乘法运算, 加法与减法统一成加法运算。

第(1)步对每一个双基线系统, 根据方程(9)需要计算p/q, 2π, $\varphi/2\pi$, $\varphi_{n+1}/2\pi$, $\varphi/(2\pi) \times (q/p)$,

共需要5次乘法运算; $\Phi_n/(2\pi)\times(q/p)-\Phi_{n+1}/2\pi$ 需要一次加法运算; 在 $(-p/2, p/2)$ 区间上计算 m_{n+1} 需要 p 次乘法、p 次加法; 求离整数最近的 m_{n+1} 需要求 p 次加法; 在 $(-P_n/2, P_n/2]$ 上计算其他 m_n 需要 GCD $(P_n, P_{n+1})-1$ 次加法; 在 $(-P_{n+1}/2, P_{n+1}/2]$ 上计算其他 m_{n+1} 需要 GCD $(P_n, P_{n+1})-1$ 次加法。总共需要进行 $p+5$ 次乘法计算和 $2p+2$GCD $(P_n, P_{n+1})-1$ 次加法计算, $n=1, 2, \cdots, N-1$, 共有 $N-1$ 个双基线系统。

第(2)步是逻辑判断过程, 确定 m_2 时需要GCD $(P_1, P_2)\times$GCD (P_2, P_3) 次判断、确定 m_3 时需要 GCD $(P_1, P_2, P_3)\times$GCD (P_3, P_4) 次判断……在确定 m_{N-1} 时需要 GCD $(P_1, P_2, \cdots, P_{N-1})\times$GCD (P_{N-1}, P_N) 次逻辑判断。

第(3)步在估计波达角时, 根据方程(6)需要3 $(N-1)+1$ 次加法运算和3次乘法运算。

N 根基线组成 $N-1$ 个双基线测向系统解模糊, 总共需要的计算量为

乘法: $(p+5)(N-1)+3$ 次;

加法: $2(N-1)(p+1)+1+2[$GCD $(P_1, P_2)+$ GCD $(L_2, L_3)+\cdots+$ GCD $(P_{N-1}, P_N)]$ 次;

判断: GCD $(P_1, P_2)\times$GCD $(P_2, P_3)+$ GCD $(P_1, P_2, P_3)\times$GCD $(P_3, P_4)+\cdots+$ GCD $(P_1, P_2, \cdots, P_{N-1})\times$GCD (P_{N-1}, P_N) 次。

如果 $N=5$, $p=4$, $q=5$, 接收阵元间的基线长度按照 $(L_1, L_2, L_3, L_4, L_5)=\left(256\frac{\lambda_0}{2}, 320\frac{\lambda_0}{2}, 400\frac{\lambda_0}{2}, 500\frac{\lambda_0}{2}, 625\frac{\lambda_0}{2}\right)$ 进行配置, 仅需要39次乘法计算、779次加法计算和7 220次逻辑判断。而按照文献[6]的方法, 利用最小均方误差准则进行二维整数搜索计算, 在 $N=5$ 时, 接收阵元的位置按 $(P_1, P_2, P_3, P_4, P_5)=\left(30\frac{\lambda_0}{2}, 75\frac{\lambda_0}{2}, 96\frac{\lambda_0}{2}, 200\frac{\lambda_0}{2}, 240\frac{\lambda_0}{2}\right)$ 进行配置, 算法大约需要进行 2×10^6 次乘法计算和 10^7 次加法计算[6]。两者相比较, 可见本文算法所需的计算量要小得多。

1.5 正确解模糊条件分析

为了正确解模糊, 关键在于利用双基线确定的模糊数必须包含一组真实的相位模糊数。根据双基线正确解模糊的条件可知[4], 鉴相误差 $\Delta\Phi_n$ 与基线长度比值 p/q 之间必须满足

$$\max(\mathrm{abs}(\Delta\Phi_n), \mathrm{abs}(\Delta\Phi_{n+1}))<\pi/(p+q)\quad n=1, 2, \cdots, N-1 \tag{10}$$

式中abs表示取绝对值运算。

整个干涉仪阵列完全由两两相邻的双基线测向系统组成, 为了使所有的双基线都能正确解模糊, 所有的鉴相误差 $\Delta\Phi_n$ 都必须满足式(10)。因此, N 根基线组成的相位干涉仪阵列正确解模糊的条件为

$$\max(\mathrm{abs}(\Delta\Phi_1), \mathrm{abs}(\Delta\Phi_2), \cdots, \mathrm{abs}(\Delta\Phi_N))<\pi/(p+q) \tag{11}$$

如果相位干涉仪的最大鉴相误差较小, 可以选取较大的互素数 p 和 q, 否则只能选取较小的互素数 p 和 q。

2 算法仿真

在只考虑鉴相误差, 不考虑信道相位不均衡误差的情况下, 利用文献[4]中的鉴相算法对常规正弦波信号鉴相后采用本算法进行相位解模糊仿真验证。至于宽带信号(如LFM 信号、BPSK 信号、QPSK 信号), 可以进行某种非线性变换, 变成具有单一频率的正弦波信号[4], 然后采用文献[4]中的鉴相算法得到鉴相值, 最后再采用本算法对其鉴相结果解模糊处理。

如图1所示, 若相位干涉仪由5个接收阵元构成, 基线长度之比 p/q 分别为4/5和5/9, 则第1种配置方案的基线长度分别为 $(L_1, L_2, L_3, L_4)=\left(64\frac{\lambda_0}{2}, 80\frac{\lambda_0}{2}, 100\frac{\lambda_0}{2}, 125\frac{\lambda_0}{2}\right)$, 第2种配置方案的基线长度分别为 $(L_1, L_2, L_3, L_4)=\left(125\frac{\lambda_0}{2}, 225\frac{\lambda_0}{2}, 405\frac{\lambda_0}{2}, 729\frac{\lambda_0}{2}\right)$, λ_0 为最高接收频率信号的波长。

下面验证正确解模糊的条件。按照式(11), 对于第1种配置, 当最大鉴相误差小于 $\pi/9$ 时, 就能完全正确解模糊; 对于第2种配置, 当最大鉴相误差小于 $\pi/14$ 时, 也能完全正确解模糊。为了验证式(11)的正确性, 仿真试验中的鉴相误差绝对值abs $(\Delta\Phi)$ 在[0, 0.70]范围内变化并相互独立, $n=1, 2, 3, 4$, 辐射目标位于 $\pi/6$ 的位置, 各进行1 000次的Monte-Carlo 试验, 可以得到正确解模糊的统计次数与最大鉴相误差的关系, 如表1所示。

表1 不同条件下正确解模糊的统计次数表

Max(abs($\Delta\Phi$))	0.05	0.10	0.15	0.20	0.25	0.30	0.35	0.40	0.45	0.50	0.55	0.60	0.65	0.70
正确次数($p/q=4/5$)	1 000	1 000	1 000	1 000	1 000	1 000	996	861	737	636	517	453	375	334
正确次数($p/q=5/9$)	1 000	1 000	1 000	1 000	906	737	573	427	333	246	198	168	130	129

从表1可以看出, 对配置1, 只要最大鉴相误差不超过0.30(略小于$\pi/9$), 解模糊就完全正确; 在最大鉴相误差大于0.35(近似为$\pi/9$)时, 会出现错误的结果。对配置2, 当最大鉴相误差不超过0.20(略小于$\pi/14$)时, 解模糊也完全正确; 当最大鉴相误差大于0.25(略大于$\pi/14$)时, 也会出现错误的结果。在各自满足式(11)的前提下, 两种配置方案都能正确解模糊, 说明式(11)是正确解模糊的充分条件。从表中也可看出, 在不满足式(11)时, 两种配置也能以一定的次数正确解模糊, 这说明式(11)给出的条件是非必要的。

在与上述配置条件相同的情况下, 假设各相位干涉仪的噪声为独立、同分布的高斯白噪声, 其信噪比在[- 20 dB, 0 dB]范围内变化, 信号采样点分别取512和1 024, 对每一种情况分别进行1 000次的Monte-Carlo试验, 可以得到正确解模糊的统计概率与信噪比的关系, 分别如图2, 3所示。图2, 3是采样点分别为512和1 024时正确解模糊的统计概率与信噪比的关系图。从图2, 3中可以看出, 随着信噪比的增加, 正确解模糊的统计概率也随之增加。对于完全能正确解模糊时所需要的最低信噪比, 配置1要小于配置2。图2中在信噪比大于- 4 dB时, 两种配置都能正确解模糊, 图3中在信噪比大于- 6 dB时, 两种配置都能正确解模糊。这说明本算法对信噪比没有苛刻的要求, 一般工程环境都能满足。

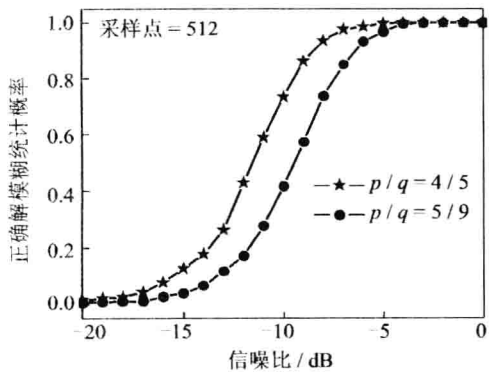

图2　正确解模糊概率与信噪比关系

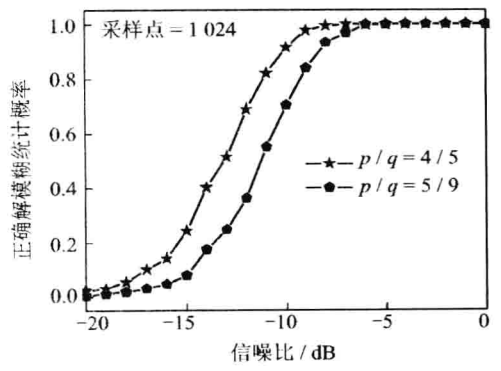

图3　正确解模糊概率与信噪比关系

3　结束语

本文对利用相位干涉仪估计波达角过程中出现的相位模糊问题进行了研究, 提出了一种基于基线比值法进行多组相位解模糊的算法, 分析了该算法的计算量。通过仿真试验, 统计了在不同信噪比条件下正确解模糊的概率。仿真结果表明, 一般的工程环境都能满足正确解模糊的技术要求。在应用相位干涉仪估计波达角时, 本文提出的相位解模糊方法具有应用价值。

参考文献:

[1] Dybdal R B. Monopulse resolution of interferometric ambiguities[J]. IEEE Trans on Aerospace and Electronic Systems, 1986, 22(2): 177-183.

[2] Messer H, Singal G, Bialy L. On the achievable DF accuracy of two kinds of active interferometers[J]. IEEE Trans on Aerospace and Electronic Systems, 1996, 32(3): 1158-1164.

[3] Kaufman M G. Radio interference phase channel combiner mod II[J]. IEEE Trans on Space Electronics and Telemetry, 1964, 10(1): 116-123.

[4] 林以猛, 刘渝, 张映南. 宽带信号的数字测向算法研究[J]. 南京航空航天大学学报, 2005, 37(3): 335-340.

[5] 贲享铁, 袁俊泉, 孙晓昶. 基于参考距离的相位差变化值的解模糊方法研究[J]. 信号处理, 2003, 19(4): 308-311.

[6] 贲享铁, 袁俊泉, 苏令华. 基于相位干涉仪阵列多组解模糊的波达角估计算法研究[J]. 电子与信息学报, 2006, 28(1): 55-59.

[7] McCormick W S, Tsui J B Y, Bakke V L. A noise insensitive solution to an ambiguity problem in spectral estimation[J]. IEEE Trans on Aerospace and Electronic Systems, 1989, 25(5): 729-732.

[8] 闵嗣鹤, 严士健. 初等数论[M]. 北京: 高等教育出版社, 2003.

A cluster-interval-based Algorithm for Optimizing Range Query in Wireless Sensor Network

Zhuang Li-jun
College of Information Science and technology
Nanjing University of Aeronautics and Astronautics
Nanjing, China
Zhuang9024@126.com

WANG Li-song
College of Information Science and technology
Nanjing University of Aeronautics and Astronautics
Nanjing, China
wls803@163.com

Abstract— **In wireless sensor network, how to use limited node energy efficiently to process data querying becomes an important research problem. We propose a cluster-based filter algorithm SFOA for range query in wireless sensor network because the data, sampled in cluster nodes, are highly similar to one another in cluster-based WSN. Its basic idea is to provide a filter for each cluster, and three filters for each node which are in the same cluster. This algorithm build cluster interval for each cluster, and inter-cluster interval for each node in the cluster to filter out the impossible clusters and nodes, which can reduce the number of nodes participating in the range query, saving nodes energy. Furthermore, the simulation experimental results indicate that, in most cases, SFOA has energy efficiency, which greatly reduce the data transmissions.**

Keywords: wireless sensor network; SFOA; range query; optimizing query; cluster interval

I. INTRODUCTION

Wireless Sensor Network (WSN) is a brand-new network technology, which develops greatly in recent years. People are taking more and more interests on it. It is composed of a large number of low-cost sensor nodes deployed in monitoring areas. Through the means of wireless communication, it forms a multi-hop and self-organizing network system, which has great future and value for human beings in the field like national defense, environmental monitoring, home automation, medical and etc.

Wireless sensors are often battery-powered, and the lifetime of the network is tied to the rate at which it consumes energy. Therefore, a key challenge in wireless sensor network is how to make use of the limited power efficiently to prolong the node life as long as possible. Moreover, in many actual applications such as environmental monitoring, the data sensor node generated (such as temperature, humidity, etc.) have high space relevance. Therefore, at present, most wireless sensor networks adopt such cluster-based network. This paper mainly research range querying. Considering the high relevance between the sensor nodes in a same cluster, we propose Sampling Filter Optimizing Algorithm(SFOA), which is based on cluster intervals in cluster-based sensor network for optimizing range query. Experiments show that, SFOA has better energy efficiency and lesser data transmission.

II. SENSOR DATA QUERY IN WSN

Because of the specific characteristics of sensor network, the data query operation often comes with the forms like "which region is below 20℃", "How many regions exceed the carbon monoxide standard"[1], "monitoring whether the humidity of every range is between 0.50 to 0.65". As wireless sensor network application is different from traditional information system, it has to obtain from the physical world. They are massive data flow, and having space relevance among these data. In cluster-based sensor network, the same cluster sampling data has high relevance. For such query form, if we collect all data to calculate the results on the server, the energy utilization will be inefficient. Especially under the circumstances that there are larger number of the query nodes, but the valid nodes are less. For this reason, some optimizing algorithms come out, which are to conserve bandwidth, reduce energy consumption and network communication.

Literature [2] presents the FILA algorithm which is a filter-based algorithm, but sometimes it will cause entire network secondary disturbance. Literature [5] presents the PREDICTOR algorithm, which, based on FILA algorithm, can avoid disturbance problem by more detailed interval-dividing. It divides sensor nodes into several intervals. But when there are large number of sensor nodes, if the interval is too large, it will cause every interval has more sensor nodes, which can not embody the effect of query optimizing; if the interval is too small, it will cause sensor nodes switching intervals frequently. Hence, this paper proposes the SFOA algorithm by building cluster intervals to optimize range query in cluster-based wireless sensor network. SFOA algorithm has more calculations on sensor node. But its energy consumption is acceptable because: (1) the energy consumption used for sensor nodes calculating is far less than that for communication. (2) The data sensed by nodes in same cluster has high relevance. The range query can save a lot of energy by filtering the clusters which do not meet the requirements with cluster interval, and the nodes with inner-cluster interval.

III. SFOA ALGORITHM

In cluster-based sensor network, SFOA algorithm reduces redundant communications by two aspects: First, we can establish cluster intervals and inner-cluster intervals by data sampling to prevent sending useless data as the high space relevance of data in a same cluster; Second, we can postpone

Foundation Items: The National Natural Science Foundation of China(60673127)

the directed query to the end of query, so as to avoid visiting most nodes which are irrelevant to the query.

Assume that there is a wireless sensor network S with n sensor nodes, i.e. S={s1, s2, ..., sn}, |S| represents the number of nodes, i.e. |S|=n. Arbitrary node si sampling data recorded as v_{si}. Sensor node may generate multidimensional data, such as temperature, humidity, light brightness, and so on. For the simplicity of discussion, we assume that the sensor acquisition data are single-dimensional. Range query RQ(a,b) is to find a result set R. Assuming that there are k nodes meeting the requirements, then $R=\{s_1,s_2,\cdots,s_k\}$, $R \subseteq S$, $|R|=k$, where $\forall v_{si} > a$ and $\forall v_{si} \le b$,(i = 1,2,..., k).

There are four phases in SFOA: initialization phase, filter generation phase, filter update phase, and result generation phase.

(1) Initialization phase

As mentioned above, in cluster-based sensor network, as soon as wireless sensor network is built, there will be self-organized cluster, selecting on node as cluster head. Then, sensor nodes will start to sampling from the network.

First, sink node send sampling message to every cluster head. Cluster head will organize all its nodes to sample data after it has received the message.

Let d denote the number of sampling times, and t_S denote the interval for sampling. After the time of $(d-1)\times t_S$, we can get the sampling space $T_{d\times n}$,

$$T_{d\times n}=\begin{bmatrix} v_{1,s_1}, v_{1,s_2}\cdots v_{1,s_n} \\ v_{2,s_1}, v_{2,s_2}\cdots v_{2,s_n} \\ \vdots \\ v_{d,s_1}, v_{d,s_2}\cdots v_{d,s_n} \end{bmatrix}$$

$v_{i,sj}$ is the sampling value of s_j node at the ith-time. The parameters d and t_s are strongly related to the practical application and energy left on the node. Their values should be adjustable at the run time. These sampling data are stored at local sensor node.

(2) Filter generation phase

After the time of $(d-1)\times t_s$, we get the sampling space. In order to reduce chanciness, guarantee that space can reflect the current situation precisely, we calculate every node's empirical value v_{pi} : $v_{pi}=\frac{(\sum_{k=1}^{d} v_{k,s_i})}{d}$, and then store v_{pi} at local node. $\min_i$ denotes the minimum data value of sampling data in the ith-cluster, $\max_i$ denotes the maximum data value of sampling data in the ith-cluster. Then the cluster interval of this cluster will be: $filter_i = (\min_i, \max_i]$.

Consider the nodes in the cluster sometime maybe very large, we divide the cluster intervals into three inner-cluster intervals based on the frequency of sampling data appearing, that is to say, finding out an interval in which the data fall into the most probably from the middle of the cluster interval. For example, we find out an interval (a, b] in which 60 percent of sampling data fall into. Probability parameters p denotes the ratio between the number of sampling data falling into interval (a, b] and the number of all sampling data. Assume there are w nodes in cluster j:

$$\frac{|\forall i,j,a < v_{i,s_j} \le b|}{(d\times w)} > p$$

$|\forall i,j,a < v_{i,s_j} \le b|$ denotes the number of sampling data that falling into (a, b], where $i=1,2,\cdots,d, j=1,2,\cdots,k$.

According the formula above, we can get the interval (a,b] in the middle of the cluster interval, educing three inner-cluster intervals as follows:

$$filter_{i,1}=(\min_i, a], \quad filter_{i,2}=(a,b], \quad filter_{i,3}=(b,\max_i]$$

.

There are several ways to determine a filter for a node, and theoretically of, each node can be assigned with a unique inner-cluster filter. The nodes information of every interval will be stored at their cluster head, and that is to say, store the information that which nodes every inner-cluster contains in the cluster head.

According to the method above, we can find out all cluster intervals and inner-cluster intervals in the whole sensor network. Assuming that the sensor network has m clusters, it will generate $3\times m$ inner-cluster filters. Its topology is shown in Figure1:

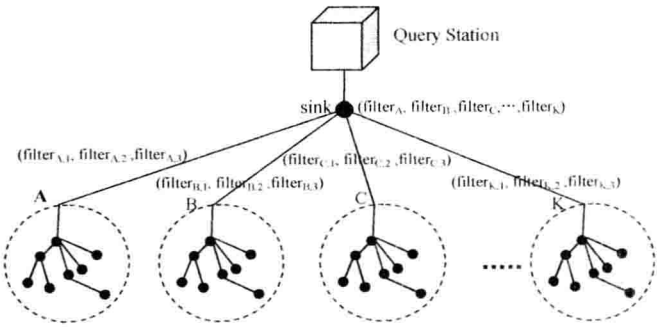

Figure1 cluster interval and inner-cluster interval in sensor network